

*Received 15 October 1998, revised 21 April 1999, accepted 28 April 1999*

TABLE 1. Relative distribution of *Shh*, *Ptc* and *Smo* mRNAs in adult rat CNS by *in situ* hybridization

Area	Shh	Ptc	Smo
Olfactory bulb	0	1+	1+
Cortex			
Parietal (layer V)	1+	0	0
Piriform	0	1+	0
Hippocampus			
Dentate granule cell layer	0	1+	4+
Basal Forebrain			
Globus pallidus	3+	0	0
Ventral pallidum	3+	1+	0
Horizontal limb diagonal band nucleus	3+	0	0
Vertical limb diagonal band nucleus	2+	0	0
Substantia Inominata	2+	0	0
Basal nucleus of Meynert	1+	0	0
Anterior amygdaloid area, dorsal part	3+	0	0
Basomedial amygdaloid nucleus	0	2+	0
Medial amygdaloid nucleus	0	3+	0
Ependymal layer of 3V	4+	1+	4+
Hypothalamus			
Magnocellular preoptic nucleus	3+	0	0
Lateral and anterior hypothalamic area	0	2+	0
Supraoptic nucleus	0	2+	0
Arcuate nucleus	0	2+	0
Ventromedial hypothalamic nucleus	0	3+	0
Thalamus			
Subthalamic nucleus	0	2+	0
Reticular thalamic nucleus	0	0	3+
Paraventricular thalamic nucleus	0	2+	0
Superior colliculus			
Superficial grey layers	0	2+	0
Cerebellum			
Purkinje cell layer	3+	4+	1+
Granule cell layer	0	2+	0
Brainstem and cranial nerve nuclei			
Oculomotor nucleus	2+	0	0
Motor trigeminal nucleus	3+	0	0
Mesencephalic trigeminal nucleus	3+	0	0
Facial nucleus	3+	2+	0
Motor vagal nucleus	3+	0	0
Hypoglossal nucleus	3+	0	0
Prepositus hypoglossal nucleus	2+	0	0
Ambiguous nucleus	2+	0	0
Medial vestibular nucleus	0	3+	0
Solitary tract nucleus	0	3+	0
Spinal cord			
Ependymal layer	0	0	1+
Ventral horn	2+	0	0
Subventricular zone	0	0	2+
Meninges	0	0	1+
Circumventricular organs			
Choroides plexuses	0	0	3+
Subcommissural organ	0	0	2+
Subfornical organ	0	0	1+
Area postrema	0	0	4+
Median eminence	0	3+	4+

Staining intensity: 0, not detectable; 1+, very low; 2+, low to moderate; 3+, moderate to strong; 4+, very strong.

*et al.*, 1996b; Oro *et al.*, 1997; Xie *et al.*, 1998) and mutations of human *Ptc* and *Smo* genes might be responsible for some primitive neuroectodermal tumours of the CNS (Vorechovsky *et al.*, 1997; Reifenberger *et al.*, 1998). The presence of *Shh*, *Ptc* and *Smo* transcripts within the Purkinje cell layer of the rat cerebellum (Traiffort *et al.*, 1998) and of medulloblastomas in *Ptc*<sup>+/−</sup> mice argues also for a role of Hh signalling in brain tumours (Goodrich *et al.*, 1997). In agreement, a role for *Shh* in controlling granule cell precursor proliferation in mice has recently been proposed (Wechsler-

Reya & Scott, 1999). In order to further characterize the potential roles exerted by this pathway in the nervous system of adult vertebrates, during diseases (Pang & Ingolia, 1998) or in the pathogenesis of brain tumours, we have performed a detailed mapping of the transcripts encoding *Shh*, *Ptc* and *Smo* in the adult rat brain and spinal cord using specific digoxigenin-labelled cRNA probes. Moreover, we have determined their pattern of expression in the developing cerebellum, and compared it with that of the transcription factor *Gli1*.

## Materials and methods

### *In situ* hybridization histochemistry

Adult male (160–220 g; Iffa Credo, France) or postnatal Wistar rats were killed by decapitation, the brain was rapidly removed from the cranium, frozen in cold isopentane maintained in liquid N<sub>2</sub> and immediately sectioned. For prenatal series, pregnant rats were killed by decapitation, the embryos were removed from amniotic membranes by caesarean section before immediate decapitation, freezing and section of the brain. Cryostat sections (20 µm) were prepared on superfrost slides/Plus (Menzel-Gläser, Germany) and stored at −80 °C until used. *In situ* hybridization (ISH) experiments were adapted from (Schaeren-Wiemers & Gerfin-Moser, 1993). Tissue sections were fixed by immersion in freshly-made 4% paraformaldehyde in 1 × phosphate-buffered saline (PBS) pH 7.4, rinsed three times in 1 × PBS, acetylated 10 min at room temperature in a mixture containing 1.33% triethanolamine, 0.2% HCl 10 N, 0.25% acetic anhydride in water and rinsed three times in 1 × PBS. Slides were prehybridized for 2 h at room temperature with 400 mL hybridization solution (50% formamide, 5 × SSC, 5 × Denhardt's solution, 500 µg/mL herring sperm DNA). Hybridization was performed overnight at 72 °C (or 68 °C in the case of riboprobes designed from species other than rat), under glass siliconized coverslips, in 150 µL of the previously-described hybridization solution containing 0.5 µg/mL digoxigenin-labelled sense or antisense riboprobes. After removal of coverslips, slides were successively washed twice for 45 min at 72 °C in 0.2 × SSC, incubated for 30 min at 37 °C in the presence of 6 µg/mL ribonuclease A, washed twice for 30 min in 0.2 × SSC at the same temperature and finally incubated for 1 h at room temperature in 0.1 M Tris-HCl pH 7.5, 0.15 M NaCl, 1% heat-inactivated normal goat serum. Immunological detection was performed by overnight incubation at 4 °C in the latest buffer supplemented with a 1:5000 dilution of a sheep antidigoxigenin antibody conjugated to alkaline phosphatase (Roche Molecular Biochemicals, France). Unfixed antibody was removed by three washes at room temperature in 0.1 M Tris-HCl pH 9.5, 0.1 M NaCl. The colourimetric detection used NBT (nitroblue tetrazolium) and BCIP (5-bromo-4-chloro-3-indolyl-phosphate) as alkaline phosphatase substrates in the presence of 0.24 mg/mL levamisole. For histological identification of brain areas, the acetylcholinesterase histochemical staining method was applied to tissue sections adjacent to those used for ISH experiments. Labelled structures are indicated in abbreviated form according to the atlas of Paxinos and Watson (Paxinos & Watson, 1986).

### RNA isolation and Northern analysis

Total RNA was isolated from adult male (160–220 g; Iffa Credo) or postnatal Wistar rats using the extraction solution RNABle (Eurobio, France). Poly(A<sup>+</sup>) RNA selection was carried out using oligo(dT)-cellulose affinity chromatography (Aviv & Leder, 1972). Three to eight micrograms of mRNA from each tissue were electrophoresed on

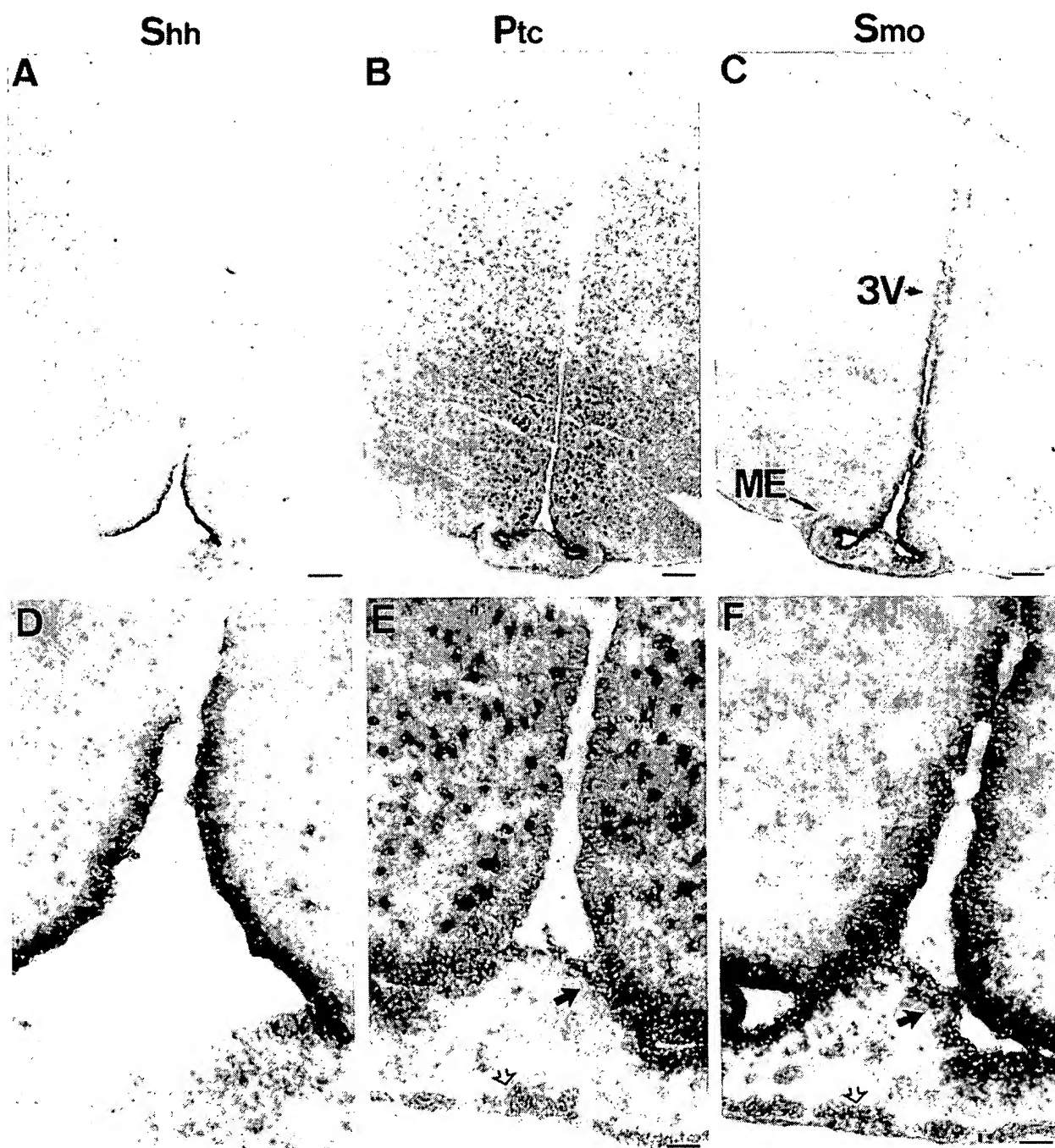


FIG. 1. *Shh*, *Ptc* and *Smo* mRNA expression at the level of the medial hypothalamic area of the adult rat suggests local Shh signalling. Frontal sections were hybridized with antisense probes specific to *Shh* (A and D), *Ptc* (B and E) or *Smo* (C and F). (A and D) *Shh* transcripts were localized in the ependymal cells lining the lower region of the ventral part of the third ventricle. (B and E) *Ptc* mRNA was highly detected in the ependymal layer (dark arrow) of the median eminence. A strong signal was observed in scattered cells localized in an area surrounding the ventral part of the lower two-thirds of the ventricle within the tuberal region of the hypothalamus. These cells were symmetrically distributed around the third ventricle. (C and F) *Smo* transcripts were highly expressed in ependymal cells lining the floor and the ventral part of the third ventricle. *Ptc* (E) and *Smo* (F) transcripts were also present in cells scattered in the fibrous connective tissue and in layers of cells that might surround capillaries in the external zone (white arrows). 3V, third ventricle; ME, median eminence. Sections corresponded to interaural levels 5.70 mm (A) and 6.44 mm (B and C). Scale bars, 200  $\mu$ m (A–C) and 50  $\mu$ m (D–F).

a formaldehyde denaturing gel containing 1% agarose, blotted overnight onto a nylon membrane (Hybond-N+, Amersham Pharmacia Biotech, France) and immobilized by heating at 80 °C for 2 h. The Northern blot was prehybridized for 2 h at 42 °C in a

solution consisting of 50% formamide, 5  $\times$  Denhart's solution, 5  $\times$  SSPE, 0.2% SDS, 0.75 mg/mL heat-denatured salmon sperm DNA. Hybridization was performed overnight at 42 °C in the same solution supplemented with 3  $\times 10^6$  cpm/mL of [ $\alpha$ - $^{32}$ P]dCTP-

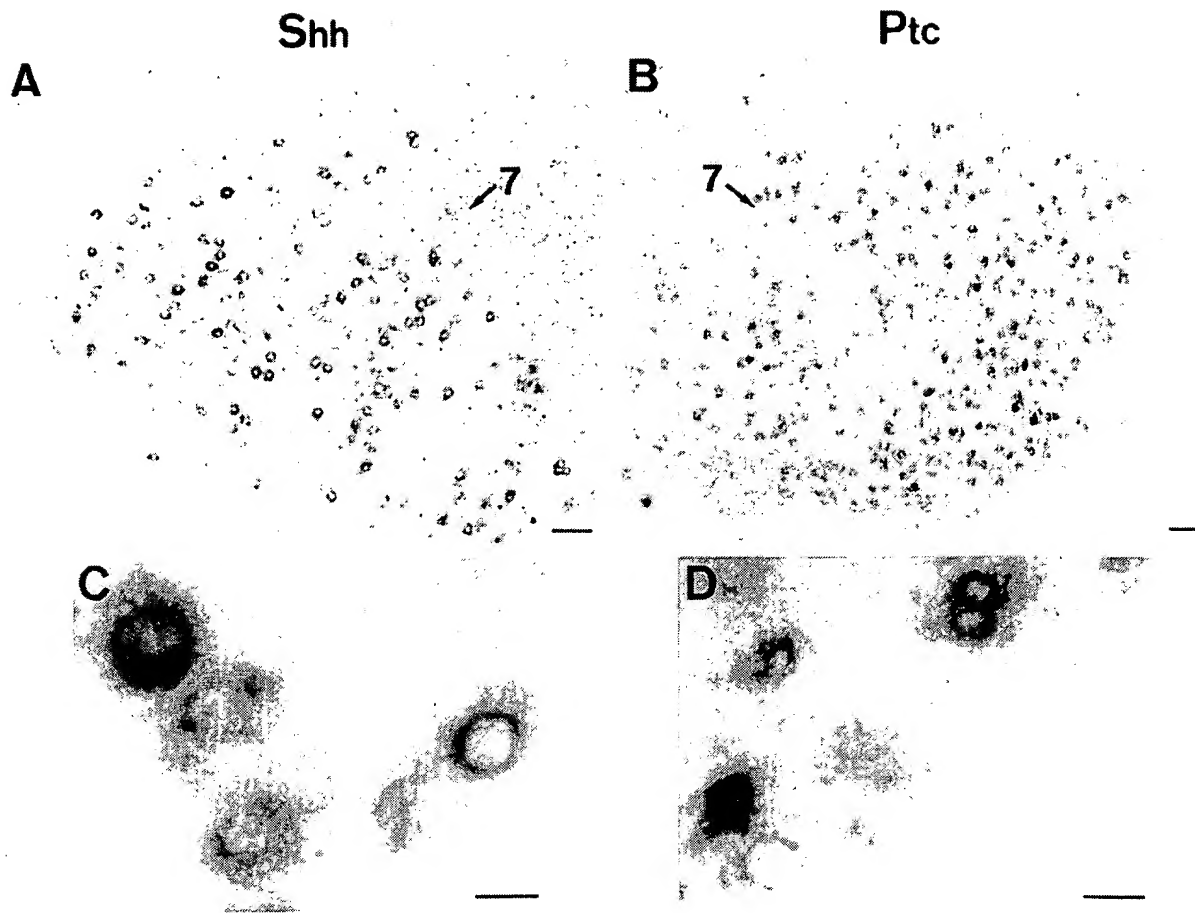


FIG. 2. *Shh* and *Ptc* mRNAs are expressed in neighbouring cells within the facial nucleus of the adult rat. *In situ* hybridization of frontal sections with *Shh* (A and C) or *Ptc* (B and D) antisense probes at the level of the facial nucleus (7). *Shh* transcripts were localized in large-sized cells, presumably motor neurons, whereas *Ptc* transcripts encoding its putative receptor were detected in a neighbouring population of smaller size cells. (C) and (D) are enlargements of facial nucleus positive cells observed from a section prepared from a different animal. Sections corresponded to interaural level  $-2.30$  mm for A and B. Scale bars,  $100\ \mu\text{m}$  (A and B) and  $20\ \mu\text{m}$  (C and D).

labelled DNA probes and washing procedure was performed as described in Traiffort *et al.*, 1998. Blot analysis was performed using a Canon Scanner (Canoscan 300).

#### RNA and DNA probe synthesis

DNA fragments of the mouse *Ptc* and *Gli1* or of the rat *Smo*, *Shh*, choline acetyltransferase (*ChAT*) and glyceraldehyde-3-phosphate dehydrogenase (*GAPDH*) genes were amplified by PCR from mouse or rat brain cDNA. Those fragments corresponded to bases 1765–3587 for the *Ptc* gene (Goodrich *et al.*, 1996), 411–2016 for *Smo* (Stone *et al.*, 1996), 678–1356 for *Shh* (Roelink *et al.*, 1994), 1–2332 for *ChAT* (Brice *et al.*, 1989), 570–1611 for *Gli1* (Walterhouse *et al.*, 1993) and 28–1056 for *GAPDH* (Tso *et al.*, 1985). PCR products of expected size were subcloned into pGEM-4Z (Promega) and sequenced to verify their identity and orientation. Sense (control) or antisense 11-UTP digoxigenin riboprobes for ISH were transcribed using T7 or SP6 RNA polymerase (Roche Molecular Biochemicals, France). Subcloned DNA was used as a template for generating [ $\alpha$ - $^{32}\text{P}$ ] dCTP-labelled specific probes for Northern blot analysis using the Nona Primer Kit (Oncor Appligene, France).

## Results

### *In situ hybridization*

*Shh*, *Ptc*, *Smo* and *Gli1* cDNAs have been cloned recently in mammals, but sensitive and specific pharmacological and biochemical tools for the identification of the encoded proteins are not yet available or fully characterized. In order to identify and characterize the expression of these developmental genes in the developing and adult brain as well as in the spinal cord of the rat, we have generated specific digoxigenin-labelled cRNA probes for each gene, and used them to analyse in detail their expression pattern by ISH. Because these gene transcripts remained detectable in adult cerebellum, and impairment of Hh signalling might be implicated in medulloblastomas, we studied their expression in the developing cerebellum.

Antisense riboprobes specific for *Shh*, *Ptc*, *Smo* and *Gli1* led to a unique pattern of cellular and regional mRNA distribution in rat brain and spinal cord. Application of antisense probes to cryostat-cut sections of frozen tissues resulted in a very low background and a highly contrasted cell labelling, as indicated by reaction products observed in a cytoplasmic rim around the cell nucleus. Sense

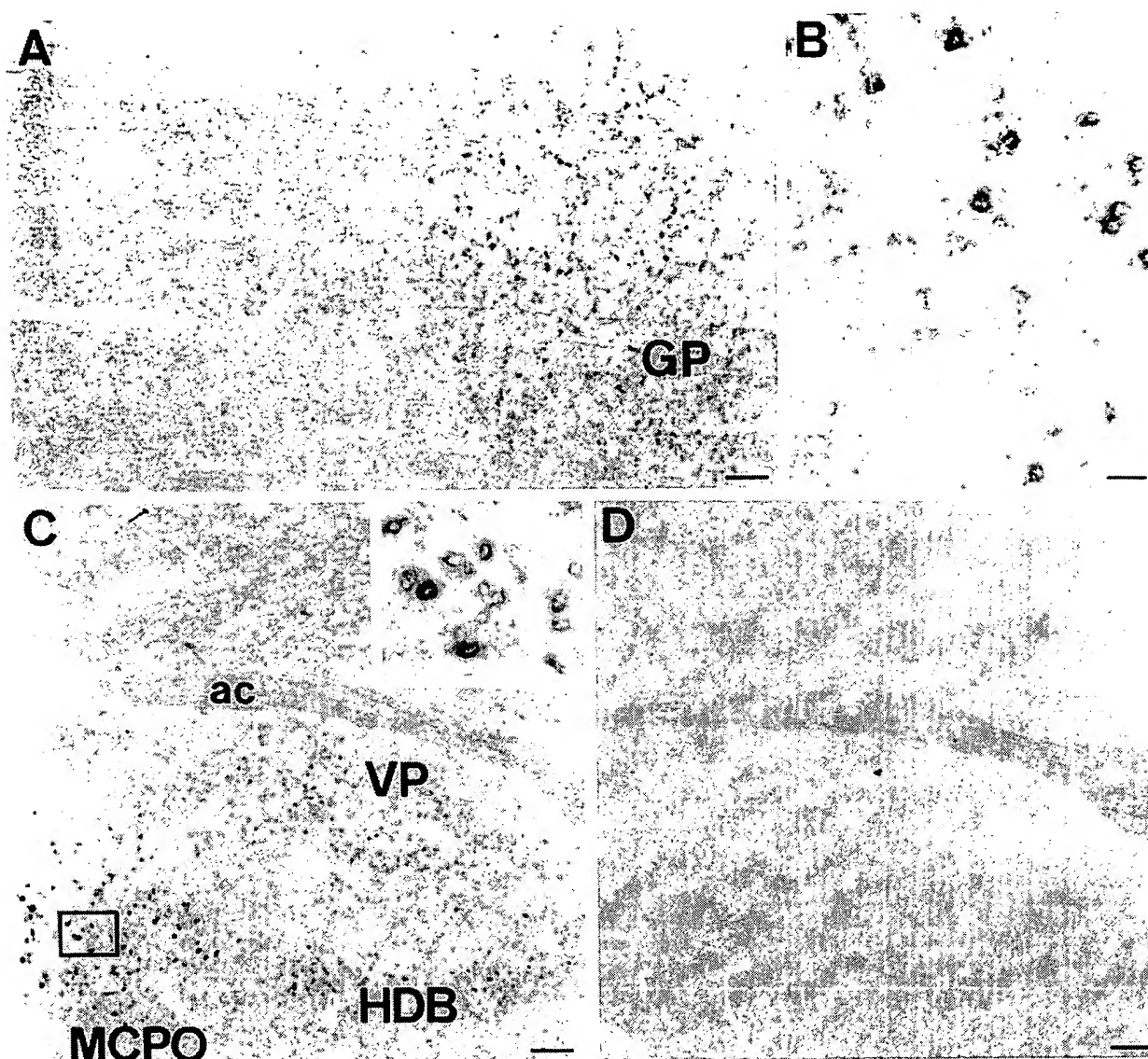


FIG. 3. Regional distribution of *Shh* mRNA in adult forebrain areas. *In situ* hybridization of frontal sections with an antisense (A–C) or a sense riboprobe (D). (A) *Shh* transcripts were detected in scattered cells of the globus pallidus (GP). (B) Enlargement from (A). (C) *Shh* transcripts are also observed in scattered cells of the ventral pallidum (VP), the horizontal limb of the diagonal band (HDB) and the magnocellular preoptic nucleus (MCPO); ac, anterior commissure. Inset, higher magnification from (C) as indicated. (D) No signal was detected with *Shh* sense riboprobe on consecutive sections. Sections corresponded to interaural level 8.60 mm. Scale bars, 200  $\mu$ m (A, C and D), 50  $\mu$ m (B).

riboprobes gave no specific signal and omission of the antisense cRNA probes from the hybridization mixtures resulted also in absence of cell staining. Also, we tested another *Ptc* riboprobe corresponding to nucleotides 136–1718 of *Ptc* gene and encoding the aminoterminal region of the mouse protein (Goodrich *et al.*, 1996), and we obtained a pattern of expression similar to that described in the present study using a probe corresponding to the carboxylterminal region. ISH experiments using *Dhh* and *Ihh* antisense riboprobes on brain and spinal cord sections gave no specific hybridization signal, further illustrating the specificity of the *Shh* signal. Comparison of relative distribution of *Shh*, *Ptc* and *Smo* transcripts in brain and spinal cord of the adult rat is summarised in Table 1 as well as in a series of low-power line drawings in Fig. 8.

#### *Shh*, *Ptc* and *Smo* transcripts are expressed at the level of the median eminence in the adult rat

We have previously observed the expression of *Shh*, *Ptc* and *Smo* transcripts within the Purkinje cell layer of the adult cerebellum (Traiffort *et al.*, 1998). Interestingly, these genes were also expressed in a complex fashion at the level of the median eminence and the ventral region of the third ventricle suggesting that they may be implicated in local signalling circuitry (Fig. 1). The median eminence, located at the base of the hypothalamus, is a structure typically devoid of neuron somata. This structure displays an internal zone comprising predominantly the supraopticohypophysial tract, and an external zone composed mainly by nerve terminals and capillaries. The neurosecretory products of these nerve endings are released into

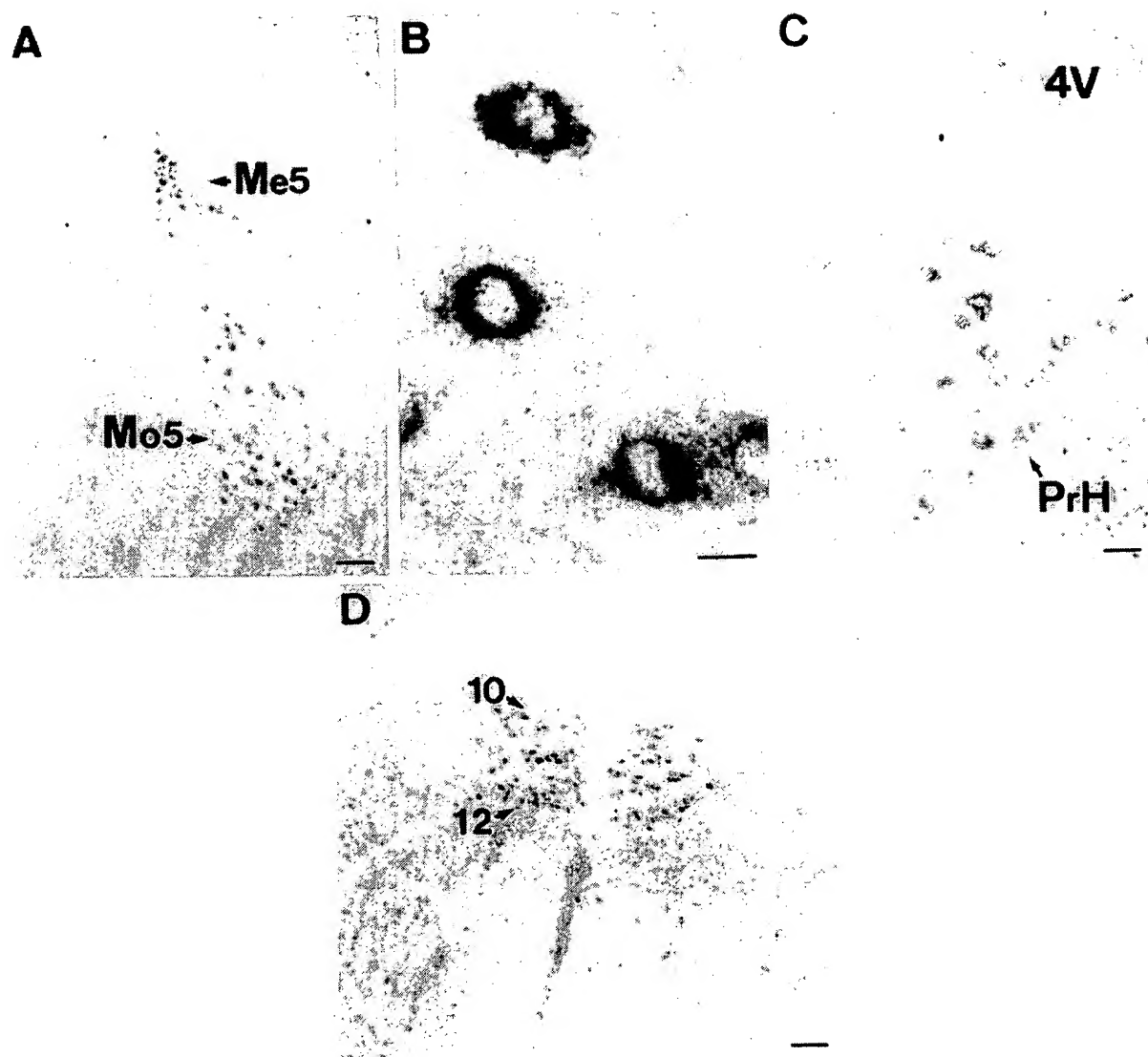


FIG. 4. Distribution of *Shh* mRNA in cranial nerve nuclei. *In situ* hybridization experiments with *Shh* antisense probe. *Shh* transcripts were detected as a thin rim of reaction products observed in large cells that might correspond to motor neurons in both motor (Mo5) (A and B) and mesencephalic (Me5) (A) trigeminal nuclei, and in prepositus hypoglossal nucleus (PrH) (C). (B) Enlargement of Mo5. (D) *Shh* mRNA is also observed in motor vagal nucleus (10) and hypoglossal nucleus (12). Frontal sections corresponded to interaural level 0.20 mm (A and B), -2.96 mm (C), -4.30 mm (D). 4V, fourth ventricle. Scale bars, 200  $\mu$ m (A and D), 20  $\mu$ m (B) and 50  $\mu$ m (C).

the capillary bed and affect the anterior pituitary functions (Page & Dovey-Hartman, 1984). Tanycytes, a specialized type of glial cells, are located in the median eminence (Ma *et al.*, 1992). We detected, by immunocytochemistry, vimentin-positive cells corresponding to tanycytes in the ventral two-thirds of the ventricle, as well as in the layer lining the median eminence. The immunoreactive processes of these cells reached the pial surface or terminated on blood vessels (data not shown). At this level, *Shh* mRNA was only detected in tanycytes lining the ventral lowest third region of the ventricle as indicated by the abrupt end of the *Shh* hybridization signal (Fig. 1A and D). *Smo* mRNA was expressed in the ventral two-thirds of the ventricle as indicated by a strong hybridization signal decorating the tanycytes' somata (Fig. 1C and F), whereas *Ptc* transcripts were faintly expressed in these cells (Fig. 1B and E). Typical ependymal cells located in the dorsal third of the ventricle were devoid of any

*Ptc* and *Shh* transcripts and expressed no, or very low, levels of *Smo* mRNAs.

*Ptc* and *Smo* signals were also strongly detected in tanycytes lining the median eminence and to a lesser extent in cells located in the internal and external zones, which may correspond to glial or ependymal cells interspersed with fibres of the hypothalamo-neurohypophyseal tract (Fig. 1B, C, E and F). Cells within the layers surrounding blood vessels in the external zone expressed both *Ptc* and *Smo*, suggesting that they might also be implicated in transduction of locally-secreted *Shh* from the tanycytes lining the third ventricle. In addition, a strong *Ptc* signal was found in cells of small to medium size scattered in a zone symmetrically distributed around the ventricle (Fig. 1B and E) and overlapping the arcuate and ventromedial hypothalamic nuclei where tanycyte processes are also observed (data not shown). Interestingly, *Smo*

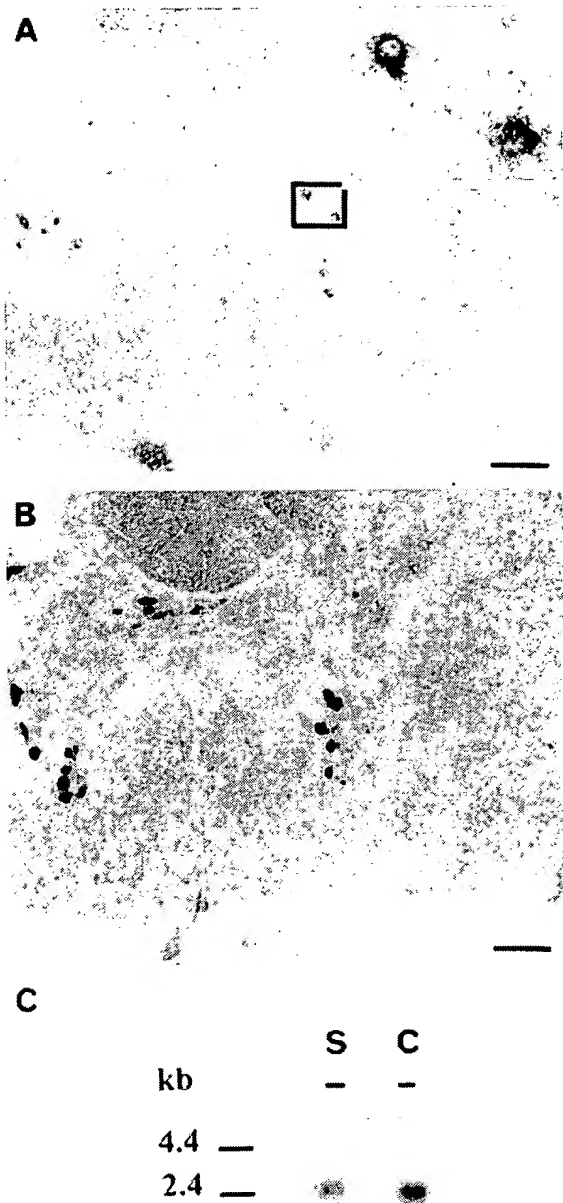


FIG. 5. Comparison of *Shh* and *ChAT* transcripts in the spinal cord. *In situ* hybridization of sections at the level of the lumbar spinal cord (A and B) with *Shh* (A) or *ChAT* (B) antisense riboprobes. (A) *Shh* probe hybridized to large cells localized in the ventral horn. Inset, higher magnification from (A) as indicated. This population of cells might correspond to motor neurons that were strongly reactive with the *ChAT* riboprobe (B). (B) Smaller cells located near the central canal were *ChAT*-positive as previously described (Butcher *et al.*, 1992). (C) Northern blot analysis of *Shh* transcripts in spinal cord (S) and cerebellum (C). A single 2.5-kb transcript was identified both from spinal cord and cerebellum. Poly (A<sup>+</sup>) RNA (8 µg) was used. The blot was exposed to X-ray films for 4 days at -80 °C with intensifying screens. The molecular size is indicated. Scale bars, 200 µm (A and B).

expression was not observed at a detectable level in these areas (Fig. 1C and F). Such a pattern of expression was found conserved for the three genes from the median eminence to the infundibular stem (data not shown).

#### *Shh* and *Ptc* transcripts are expressed in adjacent cells within the facial nucleus in the adult rat

An ISH signal with the *Shh* riboprobe was observed in large-sized cells (Fig. 2A and C) within the facial nucleus, whereas the *Ptc* riboprobe was detected in small cells (Fig. 2B and D), suggesting that, in this nucleus, *Shh* and *Ptc* transcripts would be expressed by different but adjacent cells. *Shh*-expressing cells might represent motor neurons mainly because of their size and their distribution, which were very similar to the cells positive with a *ChAT* probe (data not shown). The rather small size of cells expressing *Ptc* in this nucleus may reflect labelling of glial cells. *Smo* transcripts were not detected within the facial nucleus.

#### ISH of *Shh* in brain and spinal cord in the adult rat

In other brain areas, ISH experiments revealed the presence of *Shh*-positive cells mostly distributed in the basal ganglia and septum (Fig. 3A–C), several cranial nerve nuclei (Fig. 4) and in the spinal cord (Fig. 5A). In most of these areas, *Shh* expression probably occurred in neurons as indicated by the shape and localization of the labelled cells. A relatively high signal was observed in large cells of several cranial nerve nuclei including orofacial nuclei, i.e. the motor (Fig. 4A and B) and mesencephalic (Fig. 4A) trigeminal nuclei, the hypoglossal and the motor vagal nuclei (Fig. 4D). A moderate to strong staining occurred in medium to large cells located in the globus pallidus (Fig. 3A and B), but also in the ventral pallidum, the horizontal limb of the diagonal band nucleus, in a relatively high number of large neuron-like cells of the magnocellular preoptic nucleus of the hypothalamus (Fig. 3C), in the anterior amygdaloid area and in a region encompassing the basal nucleus of Meynert (Table 1, Fig. 8). A moderate expression of *Shh* was detected in various cholinergic basal forebrain nuclei such as the substantia innominata or the vertical limb of the diagonal band nucleus (Table 1, Fig. 8) and in the cytoplasmic region of large cells located in the ventral horn of the spinal cord (Fig. 5A) which might correspond to motor neurons. The identity of these cells was further corroborated by ISH experiments performed with the *ChAT* riboprobe (Fig. 5B). Indeed, large cells located in the ventral horn of the spinal cord, and corresponding to putative motor neurons, were clearly labelled on adjacent sections with the cholinergic marker. In agreement with the detection of *Shh* transcripts by ISH, the *Shh* cDNA probe hybridized to a 2.5-kb transcript both in spinal cord and cerebellum as indicated by Northern blot (Fig. 5C). These data clearly showed that a subset of motor neurons may express *Shh* mRNA in the adult rat. A low expression of *Shh* was detected in the cortex from the hindlimb to the lowermost border of the parietal area (Table 1, Fig. 8). Cells of medium to large size, presumably corresponding to pyramidal neurons, were sparsely and horizontally distributed in the deep layer V, whereas at postnatal day 9 (P9), *Shh* mRNA was detected in a larger population of cells that also resemble neurons (data not shown), suggesting additional roles for *Shh* signalling in developmental processes of the cerebral cortex. In the hippocampus, *Shh* mRNA was identified neither by ISH nor by Northern blot (data not shown).

#### ISH of *Ptc* in the adult rat brain

In general, *Ptc* transcripts were found in brain structures devoid of *Shh* expression (Table 1, Fig. 8) with some exceptions such as the Purkinje cell layer of the cerebellum as previously shown (Traiffort *et al.*, 1998), the median eminence region (Fig. 1B and

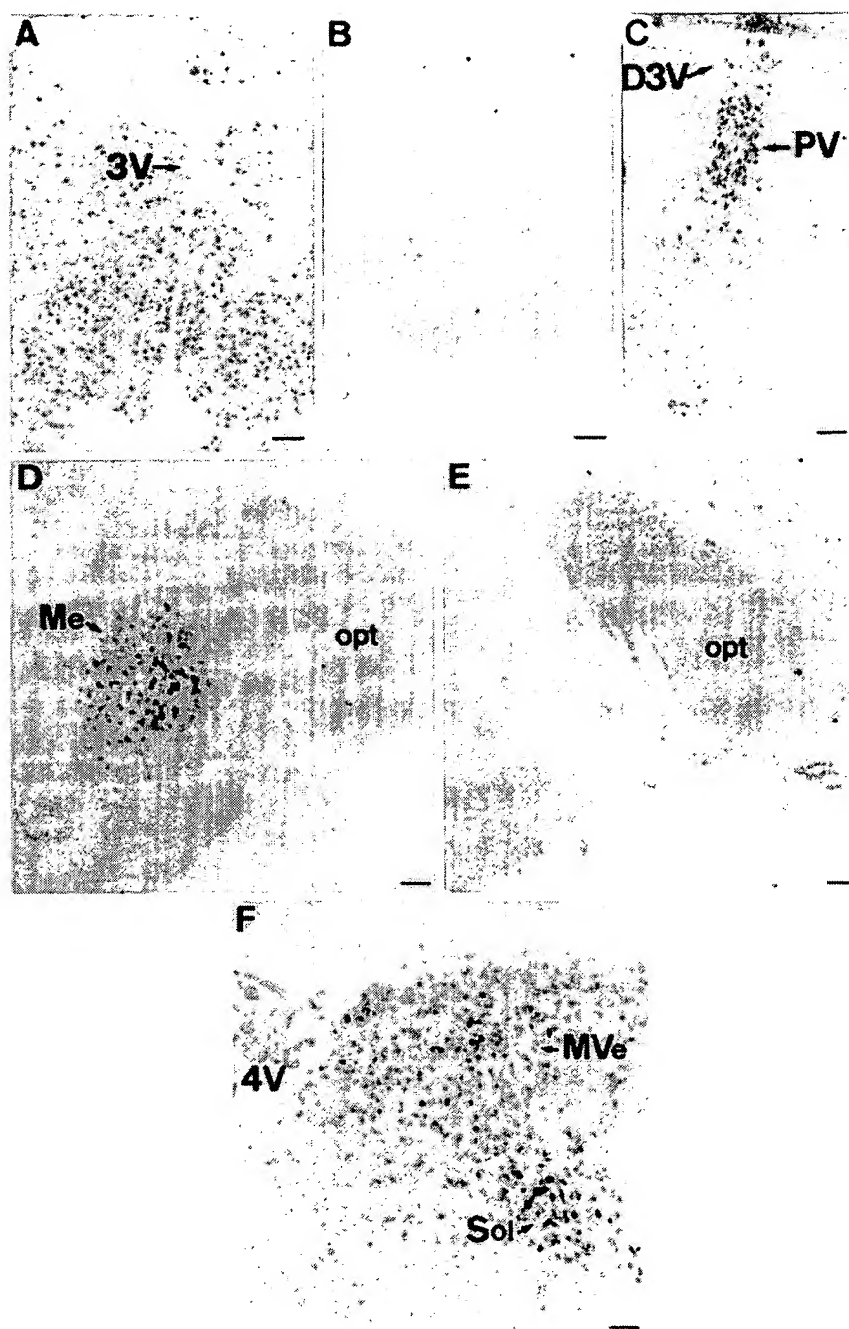


FIG. 6. Localization of *Ptc* mRNA in selected regions of the adult brain. *In situ* hybridization experiments on frontal sections with antisense (A, C, D and F) or sense (B and E) *Ptc* probes. *Ptc* transcripts were present in a large area surrounding the third ventricle (3V) and corresponding to the preoptic region of the hypothalamus (A) as well as in the paraventricular thalamic nucleus (C). These transcripts were also detected in the medial amygdaloid (Me) nucleus (D), the medial vestibular (MVe) and solitary tract nuclei (Sol) shown in (F). The *Ptc* sense riboprobe detected no signal as shown in the preoptic region of the hypothalamus (B) and medial amygdaloid nucleus (E). Sections corresponded to interaural levels 7.60 mm (A–C), 6.44 mm (D and E) and –3.30 mm (F). D3V, third ventricle, dorsal part; 4V, fourth ventricle; opt, optic tract. Scale bars, 200  $\mu$ m (A–C) and 100  $\mu$ m (D–F).

E) or the facial nucleus (Fig. 2B and D). Moderate to strong signals were observed in numerous cells of medium size located in the basomedial (Table 1, Fig. 8) and medial (Fig. 6D) amygdaloid nuclei, where two populations of labelled cells were distinguishable. *Ptc* transcripts were also moderately to strongly detected in numerous medium-sized cells distributed within the preoptic and lateral hypothalamic regions (Fig. 6A), or within the medial vestibular and solitary tract nuclei (Fig. 6F). Throughout the supraoptic nucleus, a moderate to dense *Ptc* transcript expression was observed in a heterogeneous population of medium and large cells (Table 1, Fig. 8). A moderate expression

of *Ptc* mRNA was also identified in medium-sized cells of the subthalamic nucleus (Table 1), and in a group of cells in the paraventricular thalamic nucleus (Fig. 6C) that might correspond to neurons, based on their shape and location. A low signal was detected in the granular cells of the dentate gyrus of the hippocampus (Table 1, Fig. 8), in densely packed cells of the piriform cortex, in small-sized cells of the ventral pallidum and in a high number of cells within the superior colliculus, among which a few were densely labelled in the superficial grey layers, whereas a few positive cells were also present in the deepest layers (Table 1, Fig. 8). These cells might correspond to neurons

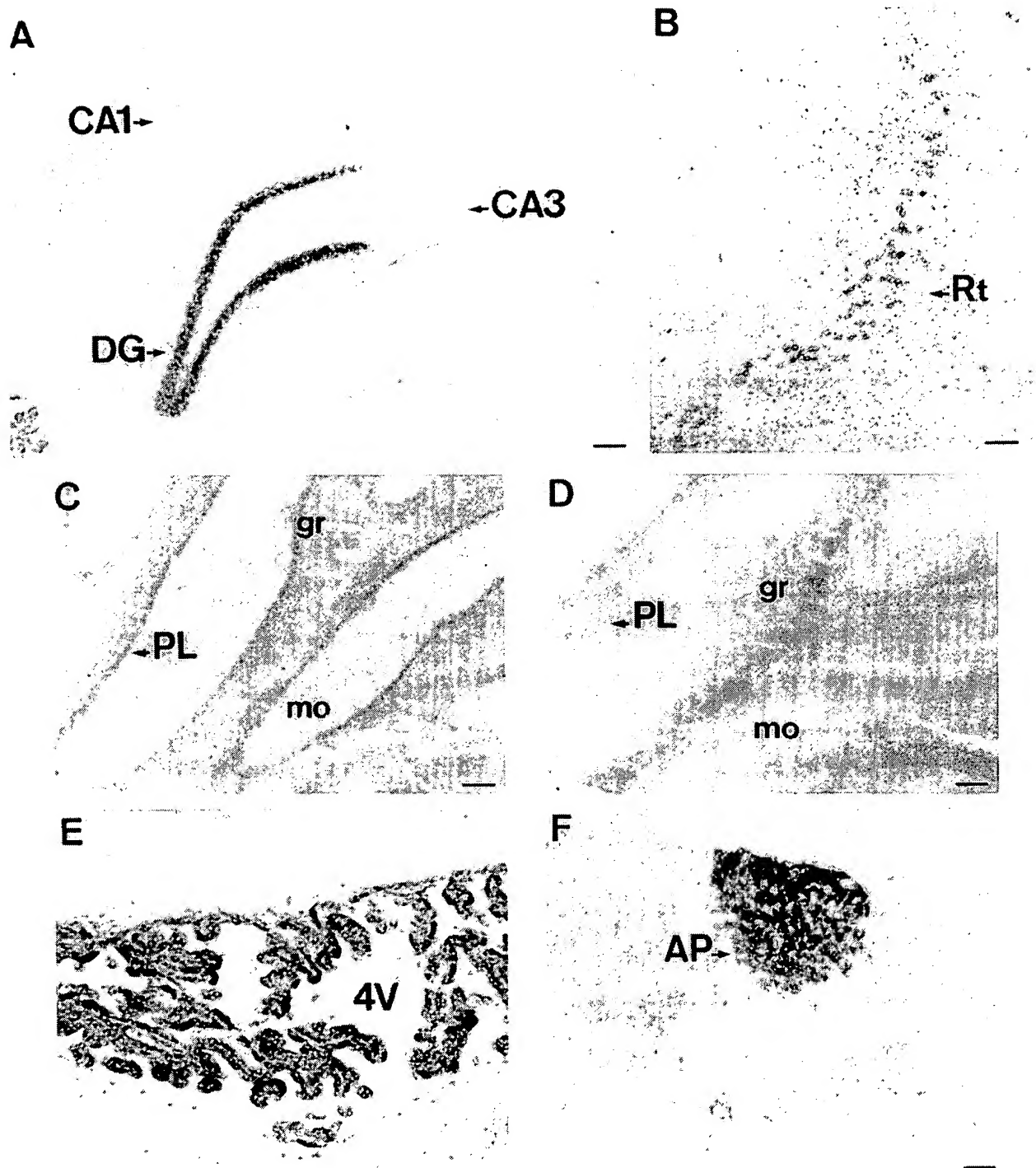
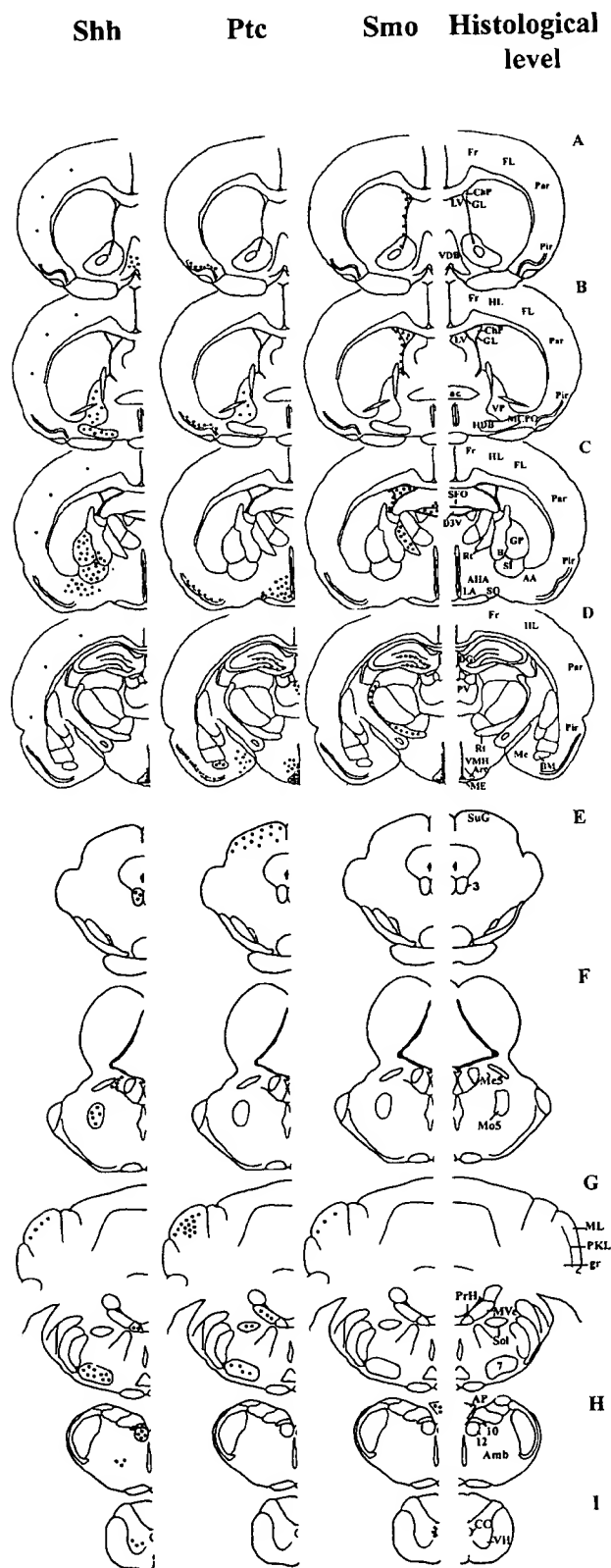


FIG. 7. Regional distribution of *Smo* mRNA in the adult brain. *In situ* hybridization experiments on frontal sections with an antisense (A-C, E and F) or sense (D) *Smo* probe. (A) A high density of transcripts was found in the granule cells of the dentate gyrus (DG), but not at the level of Ammon's horn (CA1-CA3). (B) Scattered, neuron-like cells expressed *Smo* transcripts in the reticular thalamic nucleus (Rt). (C) In the cerebellar cortex, a low signal was detected in the Purkinje cell layer (PL), but not in the granule (gr) or the molecular (mo) cell layers. The sense probe gave no detectable signal (D). *Smo* transcripts were also detected at the level of the circumventricular organs such as the choroid plexuses shown in (E) within the fourth ventricle (4V) or the area postrema (AP) visualized in (F). Sections corresponded to interaural levels 5.20 mm (A), 6.88 mm (B), -0.80 mm (C and D), -2.80 mm (E) and -4.68 mm (F). Scale bars, 200  $\mu$ m (A, C and D), 100  $\mu$ m (B and F) and 50  $\mu$ m (E).

based on their shape and location. In this latter area, neurons receive projections of the retinofugal pathway. Interestingly, a Hh

peptide might be expressed by inner rat retinal and ganglion cell layers (Jensen & Wallace, 1997; Levine *et al.*, 1997) and, in



*Drosophila*, Hh from the eye specifies neurogenesis in the developing visual centres of the brain (Huang & Kunes, 1996). *Ptc* was not identified at the level of the spinal cord by ISH.

#### ISH of *Smo* in brain and spinal cord of the adult rat

*Smo* expression was often associated to ependymal structures as exemplified for the choroid plexuses (Fig. 7E) and the subcommissural organ, which are almost exclusively composed of ependymal cells, and by the positive signal observed in a continuous layer of cells present in the subventricular zone of the lateral ventricles and extending to the subependymal layers of the olfactory part of these ventricles (Luskin, 1993), as well as in the ependymal cells lining the central canal of the spinal cord (Table 1, Fig. 8). The highest *Smo* expression occurred in the granular neurons of the dentate gyrus (Fig. 7A), in the area postrema (Fig. 7F) and in tanycytes lining the third ventricle (Fig. 1C and F). A moderate expression was seen in neuron-like cells present in the reticular thalamic nucleus (Fig. 7B). A low expression was observed in the Purkinje cell layer of the cerebellum (Fig. 7C), where *Shh* and *Ptc* have previously been reported (Traiffort *et al.*, 1998).

#### Developmental expression of genes potentially involved in *Shh* signalling in the cerebellum

The distribution pattern of transcripts encoding *Shh*, *Ptc* and *Smo* in the adult cerebellum (Traiffort *et al.*, 1998) as well as the presence of medulloblastomas in *Ptc*<sup>+/-</sup> mice led us to study more precisely the expression of these genes in embryonic and postnatal cerebellum. Expression of *Ptc* and *Smo* transcripts was analysed in a series of sagittal sections at E17, E18 and E19. Selected pictures at E18 are shown in Fig. 9 and are representative of the relative distribution observed at E17 and E19.

One of the most striking observations resides in the expression of both genes in the external germinal layer (EGL) as well as in the cerebellar neuroepithelium and in the choroid plexuses. It has been proposed that granule cell lineage arises from the EGL, a germinal zone of metencephalon origin, whereas progenitors of other cerebellar cells might arise from the cerebellar neuroepithe-

FIG. 8. Line drawings of coronal sections of the adult rat brain illustrating the comparative distributions of *Shh*, *Ptc* and *Smo* transcripts. The presence of transcripts is indicated by dark dots. These data are derived from ISH experiments conducted with *Shh*, *Ptc* and *Smo* probes as described in Figs 1–7. The right column illustrates the histological level of neuroanatomical structures. AA, anterior amygdaloid area; ac, anterior commissure; AHA, anterior hypothalamic area, anterior part; Amb, ambiguous nucleus; AP, area postrema; Arc, arcuate nucleus; B, basal nucleus of Meynert; BM, basomedial amygdaloid nucleus; CC, central canal; ChP, choroid plexus; DG, dentate gyrus; D3V, dorsal third ventricle; FL, forelimb area of the cortex; Fr, frontal cortex area; GL, germinal layer of the lateral ventricle; GP, globus pallidus; gr, granular cell layer of the cerebellar cortex; HDB, nucleus of the horizontal limb of the diagonal band; HL, hindlimb area of the cortex; LA, lateroanterior hypothalamic nucleus; LV, lateral ventricle; MCPo, magnocellular preoptic nucleus; ME, median eminence; Me, medial amygdaloid nucleus; Me5, mesencephalic trigeminal nucleus; ML, molecular layer of the cerebellar cortex; Mo5, motor trigeminal nucleus; Mve, medial vestibular nucleus; Par, parietal cortex area; Pir, piriform cortex; PKL, purkinje cell layer of the cerebellum; PrH, prepositus hypoglossal nucleus; PV, paraventricular thalamic nucleus; Rt, reticular thalamic nucleus; SFO, subfornical organ; SI, substantia innominata; SO, supraoptic nucleus; Sol, nucleus of the solitary tract; SuG, superficial grey layer of the superior colliculus; VDB, nucleus of the vertical limb of the diagonal band; VH, ventral horn of the spinal cord; VMH, ventromedial hypothalamic nucleus; VP, ventral pallidum; 3, oculomotor nucleus; 7, facial nucleus; 10, dorsal motor nucleus of vagus; 12, hypoglossal nucleus. Interaural levels (mm), A, 9.70; B, 8.70; C, 7.60; D, 6.20; E, 2.70; F, -0.16; G, -2.00; and H, -4.68.

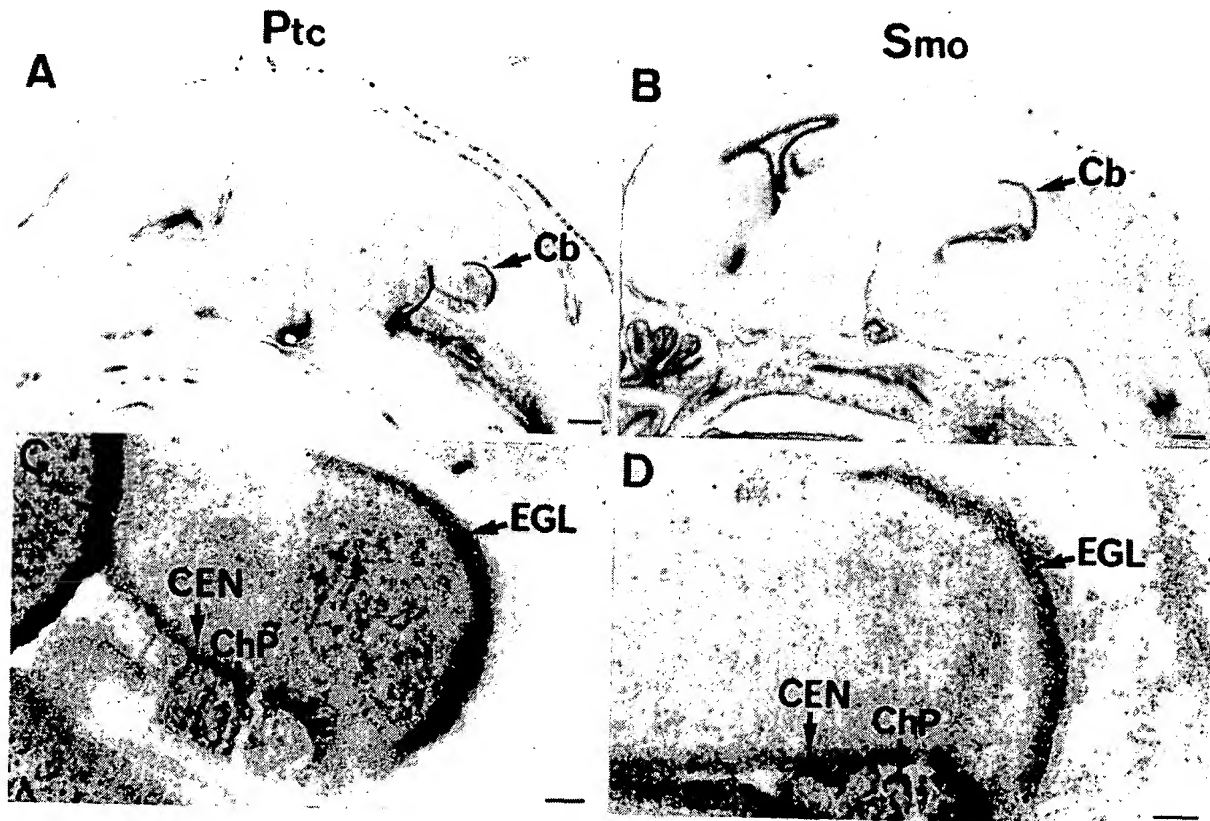


FIG. 9. Comparison of *Ptc* and *Smo* transcripts expression in E18 rat brain. *In situ* hybridization experiments were performed using *Ptc* (A and C) or *Smo* (B and D) antisense riboprobes. In the cerebellum, both mRNAs were detected in the external germinal layer (EGL) and in the cerebellar neuroepithelium (CEN). Scattered *Ptc*-expressing cells were also observed within the cerebellar primordium. *Ptc* and *Smo* transcripts were detected in choroid plexuses (ChP). Scale bars, 1 mm (A and B) and 100  $\mu$ m (C and D).

lulum or the germinal trigone (Altman, 1997; Goldowitz & Hamre, 1998). This expression pattern might suggest the potential involvement of these genes in proliferation or/and differentiation of various cerebellar progenitors. In other brain areas, a strong *Smo* expression occurred in neocortical, basal ganglia and hippocampal neuroepithelia (Fig. 9B) as well as in most other neuroepithelia (data not shown). *Ptc* expression was restricted to a limited number of neuroepithelia, such as the septal and preoptic neuroepithelia (data not shown) and the anterior pontine neuroepithelium (Fig. 9A). Nevertheless, *Ptc* transcripts were detected in various other brain areas, i.e. septal, hypothalamic, pontine and medullary areas (Fig. 9A and data not shown) and *Ptc*-positive cells were also observed within the cerebellar primordium.

Northern blot analysis performed on poly(A<sup>+</sup>) RNA from cerebellar tissues from P2 to adulthood identified the expression of 2.5, 7.9 and 3.8-kb transcripts for *Shh*, *Ptc* and *Smo*, respectively (Fig. 10). Quantification of these data by densitometric analysis and normalization for *GAPDH* showed that the level of *Smo* transcripts decreased approximately eight-fold in adult cerebellum compared with 8-day-old pups. In contrast, levels of *Ptc* and *Shh* transcripts were increased approximately three- and six-fold in the adult cerebellum compared with 2-day-old pups, respectively (Fig. 10 and data not shown).

Next we examined, in a series of sagittal sections of the postnatal cerebellum at P2, P4, P7, P9, P13, P20 and in the adult, the

spatiotemporal distribution of *Ptc*, *Smo*, *Shh* and *Gli1*, a putative transcription factor that might be involved in mediating the Hh signal (Hui *et al.*, 1994; Marigo *et al.*, 1996; Hynes *et al.*, 1997; Hardcastle *et al.*, 1998). Selected pictures showing ISH experiments of *Ptc*, *Smo* and *Gli1* at P4, P9, P20 and in the adult are shown in Fig. 11. ISH experiments performed with *Gli2* or *Gli3* riboprobes failed to identify specific signals in sagittal sections at P9 (data not shown). Interestingly, from P2 to P9, we found expression of *Ptc*, *Smo* and *Gli1* transcripts within the EGL and in the presumptive Purkinje cell layer (Fig. 11A–F). From P13 to P20, the expressions of these three genes were considerably reduced in the EGL, which ceases to exist at the end of the third postnatal week. During this period and in the adult, *Smo* and *Gli1* were faintly expressed in the Purkinje cell layer and no specific signal was found in the granular and molecular layers (Fig. 11H, I, K and L, and data not shown). In contrast, *Ptc* expression was observed in the presumptive granular cell layer from early postnatal days until adulthood, as well as within the Purkinje cell layer from P2 to adulthood, in small cells surrounding the Purkinje cells and which might represent Bergmann glial cells or a restricted population of granular cells (Fig. 11G and J, and Traiffort *et al.*, 1998). ISH experiments with *Shh* antisense probe indicated a low signal present within the Purkinje cell layer from P2 to P13 (data not shown) and we were not able to definitively identify the cell location of this signal. From P20 to adulthood, the *Shh* signal was clearly identified within the Purkinje cell bodies (Traiffort *et al.*, 1998 and data not shown). Comparison of the relative expression of *Shh*, *Ptc*,

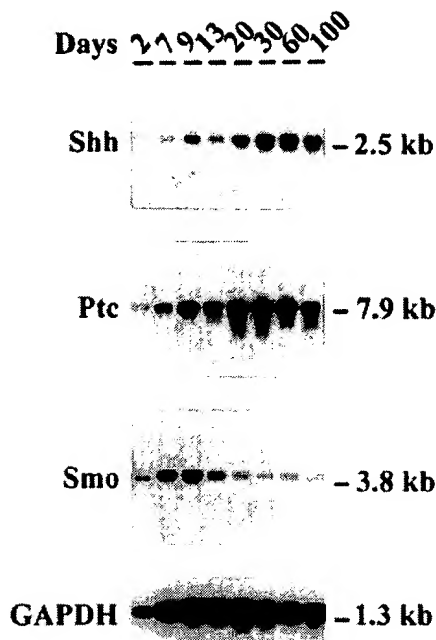


FIG. 10. Northern blot analysis of *Shh*, *Ptc* and *Smo* transcripts in the developing and adult cerebellum. Poly(A<sup>+</sup>), 8 µg per lane, was used except for day 2 (3 µg) and results were normalized to *GAPDH* expression. The same blot was hybridized successively with *Shh*, *Smo*, *Ptc* and *GAPDH* probes and exposed to X-ray films for 2–3 days at –80 °C with intensifying screens.

*Smo* and *Gli1* in the cerebellum of the P9 rat, deduced from ISH and Northern blot experiments, is reported in Table 2.

## Discussion

Sonic hedgehog exerts its biological functions through binding to *Ptc*, a multipass transmembrane protein that might form a complex with *Smo*, another membrane-associated protein sharing homology with the superfamily of G-protein-coupled receptors. Localization of the associated transcripts during embryonic development, particularly at the level of the notochord and the neural tube, has helped to further characterize Hh signalling. *Shh*, *Ptc* and *Smo* are also expressed in the adult brain of human and rat (Hahn *et al.*, 1996a; Stone *et al.*, 1996; Traiffort *et al.*, 1998). Therefore, localization of cells expressing these genes in the developing and adult brain and spinal cord will help to delineate the role of these developmental genes in the mature nervous system.

### *Shh is expressed in the adult forebrain*

In the developing brain, *Shh* specifies the fate of several ventral forebrain structures (Ericson *et al.*, 1995; Rubenstein & Beachy, 1998), and mice lacking *Shh* functions display numerous developmental defects, including a lack of ventral forebrain structures and cyclopia (Chiang *et al.*, 1996), reminiscent of holoprosencephaly in humans which is also associated with *Shh* mutations (Belloni *et al.*, 1996; Roessler *et al.*, 1996). Interestingly, we found that *Shh* mRNA, in the adult rat, is expressed predominantly within basal forebrain regions, particularly hypothalamus and basal ganglia, where it would probably affect functions associated with *Ptc* which is predominantly expressed in thalamic and hypothalamic regions.

### *Shh is expressed in adult motor neurons*

In vertebrate embryos, graded concentrations of *Shh* secreted from the floorplate and notochord induce the differentiation of ventral neural tube progenitors into motor neurons and interneurons (Roelink *et al.*, 1994; Ericson *et al.*, 1996). At mouse embryonic days 10.5–11.5, the presence of *Shh* peptides has been reported in the floorplate area, and may extend into ventrolateral regions where some motor neuron precursors express HNF-3β mRNA but not *Shh* mRNA (Marti *et al.*, 1995b) or only at low level (Bitgood & McMahon, 1995). Our results indicating the presence of *Shh* mRNA in motor neurons of the spinal cord and in several brainstem and cranial nerve nuclei in the adult and in the young animal at P13 (data not shown) are particularly intriguing, and might indicate additional roles for this molecule. Interestingly, *Ptc* transcripts were not detected in the spinal cord. Thus, localization of Hh peptides would be necessary to further delineate *Shh* functions, particularly at the level of the neuromuscular junction, because *Ptc* expression has already been detected on skeletal muscle in humans (Hahn *et al.*, 1996a).

At the supraspinal level, *Shh* was expressed in motor neurons of major cranial nerve nuclei, and most prominently in those implicated in orofacial motricity. In the facial nucleus, *Shh* from motor neurons may act on neighbouring *Ptc*-expressing cells, raising the possibility of a local signalling circuitry in this structure. *Ptc* expression was not detected in other motor nuclei suggesting that *Shh* action, if any, should be exerted on distant targets implicating a transport mechanism of the protein in the corresponding nerves. The solitary tract nucleus is implicated in gustation as well as in respiratory and cardiac rhythm control, and appears to express *Ptc* but not *Shh*. This nucleus receives afferents from the motor vagal nucleus, where *Shh* is expressed, and is connected with other respiratory structures in the brainstem, but also with the lateral hypothalamus in the forebrain which is known to modulate cardiovascular reflexes and respiratory rhythms (Feldman & Ellenberger, 1988), and where *Ptc* transcripts are also present. Thus, these results might indicate that *Shh* and *Ptc* are involved in some aspects of the regulation of these complex systems.

### *Shh, Ptc and Smo transcript distributions in the median eminence and hypothalamic areas suggest a role of Shh signalling in neuroendocrine functions*

Tanycytes of the third ventricle express various peptides such as the macrophage migration inhibitory factor (Nishibori *et al.*, 1997) or the transforming growth factor-α (Ma *et al.*, 1992), and they might be implicated in the high regenerative capacities of neurohypophysial neurons (Chauvet *et al.*, 1998). Ventricular processes of tanycytes may internalize β-endorphin present in the cerebrospinal fluid and release the peptide in the external layer of the median eminence contributing to hypothalamic hormone secretion (Bjelke & Fuxe, 1993). *Shh*, if synthesized, might be secreted by tanycytes at the level of the ventral hypothalamus and would reach either neighbouring tanycytes and cells expressing both *Ptc* and *Smo* in the median eminence or *Ptc*-expressing cells in the lateral hypothalamus. This pattern of *Shh*, *Ptc* and *Smo* expression is reminiscent of that observed during embryonic development at the level of the neural tube and responsible for ventral patterning the neuraxis.

It is tempting to speculate that *Shh* actions on these cells would affect the release of molecules in the third ventricle and the median eminence contributing to the modulation of neuroendocrine functions. *Ptc* expression within the supraoptic and the arcuate nuclei, and in several hypothalamic areas that include neurons containing releasing hormones, is also in supportive of such a role.

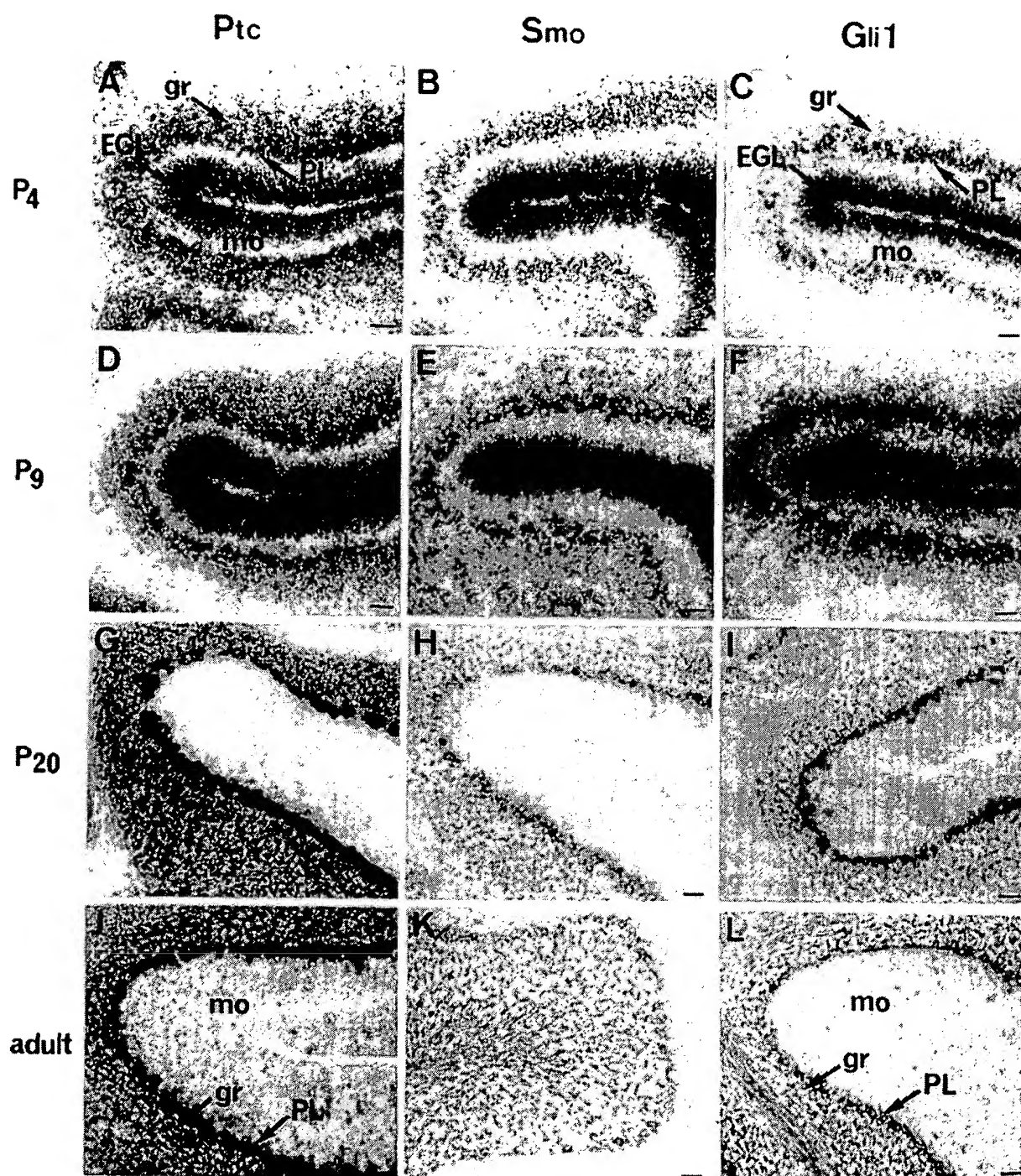


FIG. 11. Developmental expression of *Ptc*, *Smo* and *Gli1* transcripts in cerebellar cortex during postnatal development and adulthood. *In situ* hybridization experiments were performed using *Ptc* (A, D, G and J), *Smo* (B, E, H and K) or *Gli1* (C, F, I and L) antisense riboprobes on sagittal sections of P4 (A–C), P9 (D–F), P20 (G–I) and adult (J–L) rat brain. *Ptc*, *Smo* and *Gli1* transcripts were expressed in the external germinal layer as well as in the presumptive Purkinje cell layer in the developing cerebellum. In the adult, *Ptc* transcripts were observed in the granular and Purkinje cell layers, whereas *Smo* and *Gli1* transcripts were faintly detected in the Purkinje cell layer. EGL, external germinal layer; mo, molecular layer; PL, Purkinje cell layer; gr, granular cell layer. Scale bars, 50  $\mu$ m.

*Ptc* and *Smo* are colocalized only in a few areas of the adult rat brain

The overlapped distribution of *Ptc* and *Smo* transcripts found in neural folds and early neural tube was restricted to a very limited

number of adult brain areas, including the Purkinje cell layer of the cerebellar cortex, the granule cell layer of the dentate gyrus or the median eminence. The presence of *Shh* in Purkinje cells and in tanycytes of the third ventricle would argue, in these regions, for a local *Shh*-signalling circuitry involving a *Ptc*–*Smo* complex for the

TABLE 2. Localization of *Shh*, *Ptc*, *Smo* and *Gli1* transcripts in the cerebellum of P9 rats

Area	Shh	Ptc	Smo	Gli1
EGL	0	4+	4+	4+
Molecular layer	0	0	0	0
Purkinje cell layer	1+	3+	2+	2+
Granule cell layer	0	2+	0/1+	0/1+
Deep nuclei	0	2+	0	0
Fibres	0	0	0	0

EGL, external germinal layer. Staining intensity: 0, not detectable; 1+, very low; 2+, low to moderate; 3+, moderate to strong; 4+, very strong.

transduction of Shh activity, as has been proposed in developmental processes induced by Hh proteins both in *Drosophila* and in vertebrates (Beachy *et al.*, 1997; Ingham, 1998).

In most other brain areas, *Ptc* was observed in the absence of *Smo*, which might reflect either the expression of another member of the *Smo* family as yet uncharacterized or that *Ptc* may transduce Hh activities in the absence of *Smo*. Shh might also bind *Ptc2*, a homologue of *Ptc* recently identified (Motoyama *et al.*, 1998) or *Hip*, a novel Hh binding protein (Chuang & McMahon, 1999). However, our preliminary ISH experiments failed to detect the expression of *Ptc2*, either in various rat brain structures or in the developing rat brain (data not shown). Further work will also be required to delineate, in the developing and adult brain, the expression as well as the putative roles of the recently-cloned *Hip* gene. On the other hand, *Ptc* might have activities other than transducing the Hh signal, possibly mediated by its putative sterol-sensing domain and recently unraveled with the isolation of the Niemann–Pick C gene implicated in a cholesterol-trafficking disease (Carstea *et al.*, 1997; Loftus *et al.*, 1997). This domain might represent a site of interaction with the cholesterol moiety of Shh and might be important for restricting Shh action, or alternatively may be regulated by other sterols. Interestingly, cholesterol depletion in hippocampal neurons has been associated with an impairment of  $\beta$ -amyloid generation, suggesting a more direct link between sterol homeostasis and neurodegenerative diseases (Simons *et al.*, 1998).

#### *Smo* expression in brain is also found in areas devoid of *Ptc* transcripts

*Smo* displays a particular homology with the Fz (frizzled) family of serpentine receptors that might bind the Wnt family of ligands (Quirk *et al.*, 1997). This striking similarity, particularly evident in the cysteine-rich region of the aminoterminal of the protein, suggests that *Smo* may bind a member of the Wnt family. *Smo* probably acts downstream from *Ptc* and, consistent with this hypothesis, *Smo* does not bind Hh but may rather be associated with *Ptc* to form a receptor complex (Stone *et al.*, 1996). Interestingly, in *Drosophila*, *Smo* might become constitutively activated in the absence of *Ptc* (Alcedo *et al.*, 1996). In adult brain, *Smo* expression is predominantly associated with neuroepithelial and ependymal structures, mostly in areas devoid of any *Ptc* transcripts. Some of these structures, such as the ependymal layer of the lateral ventricle or of the spinal central canal, contain multipotential neuroprogenitors (Johansson *et al.*, 1999), and are in close contact with ventricular fluids that may contain an as yet uncharacterized ligand of the *Smo* protein. In the reticular thalamic nucleus, the expression of *Smo* in neuron-like cells would suggest that the protein, if translated, would influence thalamocortical transmission.

#### *Hh* signalling in the developing cerebellum and medulloblastomas

Loss of *Ptc* functions has been associated with several developmental malformations and tumours including Gorlin's syndrome, basal cell carcinomas and primitive neuroectodermal tumours of the CNS, most of which are medulloblastomas that might arise from granule cell neuroblast proliferation. Indeed, Gorlin's syndrome patients have a predisposition for certain types of CNS tumours including, notably, medulloblastomas (Goodrich & Scott, 1998). Moreover, because cerebellar medulloblastomas arise in *Ptc*<sup>+/−</sup> mice (Goodrich *et al.*, 1997), it has been postulated that mutation of the second *Ptc* allele is not necessary for their induction. Interestingly, we have identified expression of the mRNAs encoding *Ptc*, *Smo* and *Gli1* in the EGL at a period where granule cell neuroblasts proliferate and differentiate and also in the Purkinje cell layer where reside radial glial cells that might be involved in granule cell neuroblast migration in the molecular layer through their fibres (Goldowitz & Hamre, 1998). In P4 mice, *Ptc* and *Gli1*, but also *Ptc2* and *Gli2*, transcripts were abundant in the EGL, which might reflect species differences (Wechsler-Reya & Scott, 1999). These data suggest that *Ptc1*, *Ptc2* and *Smo*, but also the transcription factors *Gli1* and *Gli2*, might be implicated in the complex mechanisms involved in granule cell lineage and in the control of the granule cell population such as cell death, mitosis or secretion of trophic factors from Purkinje cells (Goldowitz & Hamre, 1998). In agreement, it has recently been proposed that the aminoterminal fragment of Shh induces proliferation of granule cell neuroblasts as well as preventing further differentiation of these neuronal cells, on primary cultures or on cerebellar slices from mice (Wechsler-Reya & Scott, 1999). In humans, *Ptc* and *Smo* mutations have been observed in sporadic primitive neuroectodermal tumours (Hahn *et al.*, 1996b; Johnson *et al.*, 1996; Vorechovsky *et al.*, 1997; Xie *et al.*, 1997; Reifenberger *et al.*, 1998). These mutations might affect the biological activities of the corresponding proteins and lead to changes in Hh target gene activities. Our ISH data in the developing cerebellum suggest that the proto-oncogene *Gli1* might be also a good candidate for such mutations in primitive neuroectodermal tumours. Indeed, this gene has been implicated in Hh signal transduction and linked to basal cell carcinomas, because overexpression of *Gli1* in *Xenopus* embryos induced tumours of the epidermis (Dahmane *et al.*, 1997). Whereas *Shh* expression was clearly identified in Purkinje cell body in the adult (Traiffort *et al.*, 1998), we were not able to definitively identify the cells expressing *Shh* in the presumptive Purkinje cell layer from the period overlapping granule cell proliferation and differentiation. Using <sup>35</sup>S-labelled antisense riboprobe, *Shh* transcripts have been detected in the cerebellum of 4-day-old mice, in the Purkinje cell layer and in the molecular layer, which consists primarily of Purkinje cell dendrites (Wechsler-Reya & Scott, 1999). The low expression of *Shh* transcripts in the developing cerebellum of the rat contrasts with its rather stronger expression in the adult cerebellum. This observation might indicate that Shh is biologically very potent in the developing cerebellum, or that another member of the Hh family is expressed during this period. However, we were not able to detect either *Dhh* or *Ihh* in rat P4 cerebellum, either by ISH or by Northern blot. Interestingly, the highest expression of *Shh* and *Ptc* is observed in the adult, where *Smo* and *Gli1* expression is the lowest. Further work will be necessary to delineate Shh functions in the adult cerebellum and understand the transduction mechanism associated with the activation of this pathway. Identification, localization and biochemical characterization of Shh peptides as well as of *Ptc* and *Smo* proteins, but also understanding the biochemical events

associated to the activation of this pathway, will be required to further address and support the potential role of these genes in brain, particularly in the adult, and their potential implications in the pathogenesis of brain tumours.

## Acknowledgements

M.R. is supported in part by a Junior group ATIPE grant from CNRS and grants from the Association Française Contre la Myopathie and the Association pour la Recherche sur le Cancer.

## Abbreviations

Dhh, desert hedgehog; EGL, external germinal layer; GAPDH glyceraldehyde-3-phosphate dehydrogenase; Ihh, indian hedgehog; ISH, *in situ* hybridization; P, postnatal day; PBS, phosphate-buffered saline; Ptc, patched; Shh, sonic hedgehog; Smo, smoothened.

## References

- Alcedo, J., Ayzenzon, M., Von Ohlen, T., Noll, M. & Hooper, J.E. (1996) The *Drosophila* smoothened gene encodes a seven-pass membrane protein, a putative receptor for the hedgehog signal. *Cell*, **86**, 221–232.
- Altman, J.B.S.A. (1997) *Development of the Cerebellum System*. CRC Press, New York.
- Aviv, H. & Leder, P. (1972) Purification of biologically active globin messenger RNA by chromatography on oligothymidylic acid-cellulose. *Proc. Natl Acad. Sci. USA*, **69**, 1408–1412.
- Beachy, P.A., Cooper, M.K., Young, K.E., vonKessler, D.P., Park, W.J., Hall, T.M.T., Leahy, D.J. & Porter, J.A. (1997) Multiple roles of cholesterol in hedgehog protein biogenesis and signaling. *Cold Spring Harb. Symp. Quant. Biol.*, **62**, 191–204.
- Belloni, E., Muenke, M., Roessler, E., Traverso, G., Siegel-Bartelt, J., Frumkin, A., Mitchell, H.F., Donis-Keller, H., Helms, C., Hing, A.V., Heng, H.H., Koop, B., Martindale, D., Rommens, J.M., Tsui, L.C. & Scherer, S.W. (1996) Identification of Sonic hedgehog as a candidate gene responsible for holoprosencephaly. *Nature Genet.*, **14**, 353–356.
- Bitgood, M.J. & McMahon, A.P. (1995) Hedgehog and Bmp genes are coexpressed at many diverse sites of cell–cell interaction in the mouse embryo. *Dev. Biol.*, **172**, 126–138.
- Bjelke, B. & Fuxe, K. (1993) Intraventricular beta-endorphin accumulates in DARPP-32 immunoreactive tanyocytes. *Neuroreport*, **5**, 265–268.
- Brice, A., Bernard, S., Raynaud, B., Ansseau, S., Coppola, T., Weber, M.J. & Mallet, J. (1989) Complete sequence of a cDNA encoding an active rat choline acetyltransferase: a tool to investigate the plasticity of cholinergic phenotype expression. *J. Neurosci. Res.*, **23**, 266–273.
- Butcher, L.L., Oh, J.D., Woolf, N.J., Edwards, R.H. & Roghani, A. (1992) Organization of central cholinergic neurons revealed by combined *in situ* hybridization histochemistry and choline-O-acetyltransferase immunocytochemistry. *Neurochem. Int.*, **21**, 429–445.
- Carstea, E.D., Morris, J.A., Coleman, K.G., Loftus, S.K., Zhang, D., Cummings, C., Gu, J., Rosenfeld, M.A., Pavan, W.J., Krizman, D.B., Nagle, J., Polymeropoulos, M.H., Sturley, S.L., Ioannou, Y.A., Higgins, M.E., Comly, M., Cooney, A., Brown, A., Kaneski, C.R., Blanchette-Mackie, E.J., Dwyer, N.K., Neufeld, E.B., Chang, T.Y., Liscum, L., Strauss III, J.F., Ohno, K., Ziegler, M., Carmi, R., Sokol, J., Markie, D., O'Neill, R.R., Van Diggelen, O.P., Ellender, M., Patterson, M.C., Brady, R.O., Vanier, M.T., Pentchev, P.G. & Tagle, D.A. (1997) Niemann–Pick C1 disease gene: homology to mediators of cholesterol homeostasis. *Science*, **277**, 228–231.
- Chauvet, N., Prieto, M. & Alonso, G. (1998) Tanyocytes present in the adult rat mediobasal hypothalamus support the regeneration of monoaminergic axons. *Exp. Neurol.*, **151**, 1–13.
- Chiang, C., Litingtung, Y., Lee, E., Young, K.E., Corden, J.L., Westphal, H. & Beachy, P.A. (1996) Cyclopia and defective axial patterning in mice lacking Sonic hedgehog gene function. *Nature*, **383**, 407–413.
- Chuang, P.T. & McMahon, A.P. (1999) Vertebrate hedgehog signalling modulated by induction of a hedgehog-binding protein. *Nature*, **397**, 617–621.
- Dahmane, N., Lee, J., Robins, P., Heller, P. & Ruiz i Altaba, A. (1997) Activation of the transcription factor Gli1 and the Sonic hedgehog signalling pathway in skin tumours. *Nature*, **389**, 876–881.
- Ericson, J., Morton, S., Kawakami, A., Roelink, H. & Jessell, T.M. (1996) Two critical periods of Sonic Hedgehog signaling required for the specification of motor neuron identity. *Cell*, **87**, 661–673.
- Ericson, J., Muhr, J., Placzek, M., Lints, T., Jessell, T.M. & Edlund, T. (1995) Sonic hedgehog induces the differentiation of ventral forebrain neurons: a common signal for ventral patterning within the neural tube. *Cell*, **81**, 747–756.
- Ericson, J., Rashbass, P., Schedl, A., Brenner-Morton, S., Kawakami, A., vanHeyningen, V., Jessell, T.M. & Briscoe, J. (1997) Pax6 controls progenitor cell identity and neuronal fate in response to graded shh signaling. *Cell*, **90**, 169–180.
- Feldman, J.L. & Ellenberger, H.H. (1988) Central coordination of respiratory and cardiovascular control in mammals. *Annu. Rev. Physiol.*, **50**, 593–606.
- Goldowitz, D. & Hamre, K. (1998) The cells and molecules that make a cerebellum. *Trends Neurosci.*, **21**, 375–382.
- Goodrich, L.V., Johnson, R.L., Milenkovic, L., McMahon, J.A. & Scott, M.P. (1996) Conservation of the hedgehog/patched signaling pathway from flies to mice: induction of a mouse patched gene by Hedgehog. *Genes Dev.*, **10**, 301–312.
- Goodrich, L.V., Milenkovic, L., Higgins, K.M. & Scott, M.P. (1997) Altered neural cell fates and medulloblastoma in mouse patched mutants. *Science*, **277**, 1109–1113.
- Goodrich, L.V. & Scott, M.P. (1998) Hedgehog and patched in neural development and disease. *Neuron*, **21**, 1243–1257.
- Hahn, H., Christiansen, J., Wicking, C., Zaphiropoulos, P.G., Chidambaram, A., Gerrard, B., Vorechovsky, I., Bale, A.E., Toftgard, R., Dean, M. & Wainwright, B. (1996a) A mammalian patched homolog is expressed in target tissues of sonic hedgehog and maps to a region associated with developmental abnormalities. *J. Biol. Chem.*, **271**, 12125–12128.
- Hahn, H., Wicking, C., Zaphiropoulos, P.G., Gailani, M.R., Shanley, S., Chidambaram, A., Vorechovsky, I., Holmberg, E., Unden, A.B., Gillies, S., Negus, K., Smyth, I., Pressman, C., Leffell, D.J., Gerrard, B., Goldstein, A.M., Dean, M., Toftgard, R., Chenevix-Trench, G., Wainwright, B. & Bale, A.E. (1996b) Mutations of the human homolog of drosophila patched in the nevus basal cell carcinoma syndrome. *Cell*, **85**, 841–851.
- Hammerschmidt, M., Brook, A. & McMahon, A.P. (1997) The world according to hedgehog. *Trends Genet.*, **13**, 14–21.
- Hardcastle, Z., Mo, R., Hui, C.C. & Sharpe, P.T. (1998) The Shh signalling pathway in tooth development: defects in Gli2 and Gli3 mutants. *Dev.*, **125**, 2803–2811.
- van den Heuvel, M. & Ingham, P.W. (1996) Smoothened encodes a receptor-like serpentine protein required for hedgehog signalling. *Nature*, **382**, 547–551.
- Huang, Z. & Kunes, S. (1996) Hedgehog, transmitted along retinal axons, triggers neurogenesis in the developing visual centers of the *Drosophila* brain. *Cell*, **86**, 411–422.
- Hui, C.C., Slusarski, D., Platt, K.A., Holmgren, R. & Joyner, A.L. (1994) Expression of three mouse homologs of the *Drosophila* segment polarity gene cubitus interruptus, Gli, Gli-2, and Gli-3, in ectoderm- and mesoderm-derived tissues suggests multiple roles during postimplantation development. *Dev. Biol.*, **162**, 402–413.
- Hynes, M., Porter, J.A., Chiang, C., Chang, D., Tessier-Lavigne, M., Beachy, P.A. & Rosenthal, A. (1995) Induction of midbrain dopaminergic neurons by Sonic hedgehog. *Neuron*, **15**, 35–44.
- Hynes, M., Stone, D.M., Dowd, M., Pitts-Meek, S., Goddard, A., Gurney, A. & Rosenthal, A. (1997) Control of cell pattern in the neural tube by the zinc finger transcription factor and oncogene Gli-1. *Neuron*, **19**, 15–26.
- Ingham, P.W. (1998) Transducing Hedgehog: the story so far. *EMBO J.*, **17**, 3505–3511.
- Jensen, A.M. & Wallace, V.A. (1997) Expression of Sonic hedgehog and its putative role as a precursor cell mitogen in the developing mouse retina. *Development*, **124**, 363–371.
- Johansson, C.B., Momba, S., Clarke, D.L., Risling, M., Lendahl, U. & Frisen, J. (1999) Identification of a neural stem cell in the adult mammalian central nervous system. *Cell*, **96**, 25–34.
- Johnson, R.L., Rothman, A.L., Xie, J., Goodrich, L.V., Bare, J.W., Bonifas, J.M., Quinn, A.G., Myers, R.M., Cox, D.R., Epstein, E.H. Jr & Scott, M.P. (1996) Human homolog of patched, a candidate gene for the basal cell nevus syndrome. *Science*, **272**, 1668–1671.
- Kelley, R.I., Roessler, E., Hennekam, R.C.M., Feldman, G.I., Kosaki, K., Jones, M.C., Palumbos, J.C. & Muenke, M. (1996) Holoprosencephaly in RSH/Smith–Lemli–Opitz syndrome: Does abnormal cholesterol metabolism affect the function of Sonic Hedgehog? *Am. J. Med. Genet.*, **66**, 478–484.
- Levine, E.M., Roelink, H., Turner, J. & Reh, T.A. (1997) Sonic hedgehog promotes rod photoreceptor differentiation in mammalian retinal cells *in vitro*. *J. Neurosci.*, **17**, 6277–6288.

- Loftus, S.K., Morris, J.A., Carstea, E.D., Gu, J.Z., Cummings, C., Brown, A., Ellison, J., Ohno, K., Rosenfeld, M.A., Tagle, D.A., Pentchev, P.G. & Pavan, W.J. (1997) Murine model of Niemann-Pick C disease: mutation in a cholesterol homeostasis gene. *Science*, **277**, 232–235.
- Luskin, M.B. (1993) Restricted proliferation and migration of postnatally generated neurons derived from the forebrain subventricular zone. *Neuron*, **11**, 173–189.
- Ma, Y.J., Junier, M.P., Costa, M.E. & Ojeda, S.R. (1992) Transforming growth factor- $\alpha$  gene expression in the hypothalamus is developmentally regulated and linked to sexual maturation. *Neuron*, **9**, 657–670.
- Marigo, V., Johnson, R.L., Vortkamp, A. & Tabin, C.J. (1996) Sonic hedgehog differentially regulates expression of GLI and GLI3 during limb development. *Dev. Biol.*, **180**, 273–283.
- Marti, E., Bumcrot, D.A., Takada, R. & McMahon, A.P. (1995a) Requirement of 19K form of Sonic hedgehog for induction of distinct ventral cell types in CNS explants. *Nature*, **375**, 322–325.
- Marti, E., Takada, R., Bumcrot, D.A., Sasaki, H. & McMahon, A.P. (1995b) Distribution of Sonic hedgehog peptides in the developing chick and mouse embryo. *Development*, **121**, 2537–2547.
- Matise, M.P., Epstein, D.J., Park, H.L., Platt, K.A. & Joyner, A.L. (1998) Gli2 is required for induction of floor plate and adjacent cells, but not most ventral neurons in the mouse central nervous system. *Development*, **125**, 2759–2770.
- Miao, N.N., Wang, M., Ott, J.A.D., Alessandro, S., Woolf, T.M., Bumcrot, D.A., Mahanthappa, N.K. & Pang, K. (1997) Sonic hedgehog promotes the survival of specific CNS neuron populations and protects these cells from toxic insult in vitro. *J. Neurosci.*, **17**, 5891–5899.
- Motoyama, J., Takabatake, T., Takeshima, K. & Hui, C. (1998) Ptc2, a second mouse Patched gene is co-expressed with Sonic hedgehog. *Nat. Genet.*, **18**, 104–106.
- Nishibori, M., Nakaya, N., Mori, S. & Saeki, K. (1997) Immunohistochemical localization of macrophage migration inhibitory factor (MIF) in tanyctes, subcommissural organ and choroid plexus in the rat brain. *Brain Res.*, **758**, 259–262.
- Oro, A.E., Higgins, K.M., Hu, Z., Bonifas, J.M., Epstein, E.H. Jr & Scott, M.P. (1997) Basal cell carcinomas in mice overexpressing sonic hedgehog. *Science*, **276**, 817–821.
- Page, R.B. & Dovey-Hartman, B.J. (1984) Neurohemal contact in the internal zone of the rabbit median eminence. *J. Comp. Neurol.*, **226**, 274–288.
- Pang, K. & Ingolia, T.D. (1998) Sonic hedgehog protein: a novel approach to the treatment of neurodegenerative disorders. *CNS Drugs*, **9**, 253–259.
- Paxinos, G. & Watson, C. (1986) *The Rat Brain in Stereotaxic Coordinates*. Academic Press, London.
- Pepinsky, R.B., Zeng, C., Wen, D., Rayhorn, P., Baker, D.P., Williams, K.P., Bixler, S.A., Ambrose, C.M., Garber, E.A., Miatkowski, K., Taylor, F.R., Wang, E.A. & Galdes, A. (1998) Identification of a palmitic acid-modified form of human Sonic hedgehog. *J. Biol. Chem.*, **273**, 14037–14045.
- Quirk, J., vandenHeuvel, M., Henrique, D., Marigo, V., Jones, T.A., Tabin, C. & Ingham, P.W. (1997) The smoothened gene and hedgehog signal transduction in Drosophila and vertebrate development. *Cold Spring Harbor Symposia Quantitative Biol.*, **62**, 217–226.
- Reifenberger, J., Wolter, M., Weber, R.G., Megahed, M., Ruzicka, T., Lichter, P. & Reifenberger, G. (1998) Missense mutations in SMOH in sporadic basal cell carcinomas of the skin and primitive neuroectodermal tumors of the central nervous system. *Cancer Res.*, **58**, 1798–1803.
- Roelink, H., Augsburger, A., Heemskerk, J., Korzh, V., Norlin, S., Ruiz i Altaba, A., Tanabe, Y., Placzek, M., Edlund, T., Jessell, T.M. & et al. (1994) Floor plate and motor neuron induction by vhh-1, a vertebrate homolog of hedgehog expressed by the notochord. *Cell*, **76**, 761–775.
- Roessler, E., Belloni, E., Gaudenz, K., Jay, P., Berta, P., Scherer, S.W., Tsui, L.C. & Muenke, M. (1996) Mutations in the human Sonic Hedgehog gene cause holoprosencephaly. *Nat. Genet.*, **14**, 357–360.
- Rubenstein, J.L.R. & Beachy, P.A. (1998) Patterning of the embryonic forebrain. *Curr. Op. Neurobiol.*, **8**, 18–26.
- Sasaki, H., Hui, C., Nakafuku, M. & Kondoh, H. (1997) A binding site for Gli proteins is essential for HNF-3 $\beta$  floor plate enhancer activity in transgenics and can respond to Shh in vitro. *Development*, **124**, 1313–1322.
- Schaeren-Wiemers, N. & Gerfin-Moser, A. (1993) A single protocol to detect transcripts of various types and expression levels in neural tissue and cultured cells: in situ hybridization using digoxigenin-labelled cRNA probes. *Histochemistry*, **100**, 431–440.
- Simons, M., Keller, P., De Strooper, B., Beyreuther, K., Dotti, C.G. & Simons, K. (1998) Cholesterol depletion inhibits the generation of beta-amyloid in hippocampal neurons. *Proc. Natl Acad. Sci. USA*, **95**, 6460–6464.
- Stone, D.M., Hynes, M., Armanini, M., Swanson, T.A., Gu, Q., Johnson, R.L., Scott, M.P., Pennica, D., Goddard, A., Phillips, H., Noll, M., Hooper, J.E., de Sauvage, F. & Rosenthal, A. (1996) The tumour-suppressor gene patched encodes a candidate receptor for Sonic hedgehog. *Nature*, **384**, 129–134.
- Traiffort, E., Charytoniuk, D.A., Faure, H. & Ruat, M. (1998) Regional distribution of sonic hedgehog, patched, and smoothened mRNA in the adult rat brain. *J. Neurochem.*, **70**, 1327–1330.
- Tso, J.Y., Sun, X.H., Kao, T.H., Reece, K.S. & Wu, R. (1985) Isolation and characterization of rat and human glyceraldehyde-3-phosphate dehydrogenase cDNAs: genomic complexity and molecular evolution of the gene. *Nucl. Acids Res.*, **13**, 2485–2502.
- Vorechovsky, I., Tingby, O., Hartman, M., Stromberg, B., Nister, M., Collins, V.P. & Toftgard, R. (1997) Somatic mutations in the human homologue of Drosophila patched in primitive neuroectodermal tumours. *Oncogene*, **15**, 361–366.
- Walterhouse, D., Ahmed, M., Slusarski, D., Kalamaras, J., Boucher, D., Holmgren, R. & Iannaccone, P. (1993) Gli, a zinc finger transcription factor and oncogene, is expressed during normal mouse development. *Dev. Dyn.*, **196**, 91–102.
- Wang, M.Z., Jin, P., Bumcrot, D.A., Marigo, V., McMahon, A.P., Wang, E.A., Woolf, T. & Pang, K. (1995) Induction of dopaminergic neuron phenotype in the midbrain by Sonic hedgehog protein. *Nat. Med.*, **1**, 1184–1188.
- Wechsler-Reya, R.J. & Scott, M. (1999) Control of neuronal precursor proliferation in the cerebellum by Sonic Hedgehog. *Neuron*, **22**, 103–114.
- Xie, J., Johnson, R.L., Zhang, X., Bare, J.W., Waldman, F.M., Cogen, P.H., Menon, A.G., Warren, R.S., Chen, L.C., Scott, M.P. & Epstein, E.H. (1997) Mutations of the patched gene in several types of sporadic extracutaneous tumors. *Cancer Res.*, **57**, 2369–2372.
- Xie, J., Murone, M., Luoh, S.M., Ryan, A., Gu, Q., Zhang, C., Bonifas, J.M., Lam, C.W., Hynes, M., Goddard, A., Rosenthal, A., Epstein, E.H. Jr & de Sauvage, F.J. (1998) Activating smoothened mutations in sporadic basal-cell carcinoma. *Nature*, **391**, 90–92.
- Ye, W., Shimamura, K., Rubenstein, J.L., Hynes, M.A. & Rosenthal, A. (1998) FGF and Shh signals control dopaminergic and serotonergic cell fate in the anterior neural plate. *Cell*, **93**, 755–766.